

## Southern Illinois University Carbondale OpenSIUC

---

Publications

Department of Physics

---

5-2002

# Magnetic and Electronic Transport Properties of $\text{Yb}_x\text{Ca}_{1-x}\text{MnO}_3$ Compounds

Yongquan Guo

*Southern Illinois University Carbondale*

Sujoy Roy

*Southern Illinois University Carbondale*

Naushad Ali

*Southern Illinois University Carbondale*

Mauro R. Sardela

*University of Illinois at Urbana-Champaign*

Follow this and additional works at: [http://opensiuc.lib.siu.edu/phys\\_pubs](http://opensiuc.lib.siu.edu/phys_pubs)

© 2002 American Institute of Physics

Published in *Journal of Applied Physics*, Vol. 91 No. 10 (2002) at doi: [10.1063/1.1451702](https://doi.org/10.1063/1.1451702)

---

### Recommended Citation

Guo, Yongquan, Roy, Sujoy, Ali, Naushad and Sardela, Mauro R. "Magnetic and Electronic Transport Properties of  $\text{Yb}_x\text{Ca}_{1-x}\text{MnO}_3$  Compounds." (May 2002).

This Article is brought to you for free and open access by the Department of Physics at OpenSIUC. It has been accepted for inclusion in Publications by an authorized administrator of OpenSIUC. For more information, please contact [opensiuc@lib.siu.edu](mailto:opensiuc@lib.siu.edu).

## Magnetic and electronic transport properties of $\text{Yb}_x\text{Ca}_{1-x}\text{MnO}_3$ compounds

Yongquan Guo, Sujoy Roy, and Naushad Ali<sup>a)</sup>

*Department of Physics, Southern Illinois University, Carbondale, Illinois 62901*

Mauro R. Sardela, Jr.

*Center for Microanalysis of Materials, Materials Research Laboratory, University of Illinois, 104 S. Goodwin Avenue, Urbana, Illinois 61801*

The polycrystalline  $\text{Yb}_x\text{Ca}_{1-x}\text{MnO}_3$  ( $x=0.1,0.2$ ) were studied by x-ray powder diffraction, magnetic, and electrical resistivity measurements. The  $\text{Yb}_x\text{Ca}_{1-x}\text{MnO}_3$  crystallizes in an orthogonally distorted perovskite structure, and shows the ferromagnetic ordering with  $T_C$  more than 110 K. However, the field dependence of magnetization and electrical resistivity exhibits very complicated behavior. A magnetic field induced insulator–metal transition has been found in the  $\text{Yb}_{0.2}\text{Ca}_{0.8}\text{MnO}_3$  compound. In addition, the large asymmetry in magnetization and resistivity hysteresis loops has been observed in this compound at 10 K, which might be due to the charge ordering and magnetocrystalline anisotropy. © 2002 American Institute of Physics.

[DOI: 10.1063/1.1451702]

The recent discovery of colossal magnetoresistance in the alkaline-earth-doped light rare earth manganese oxides with the  $\text{ABO}_3$  perovskite structure has attracted renewed interest due to its scientific significance and potential applications.<sup>1</sup> The underlying physics of those phenomena has been interpreted in terms of the double-exchange mechanism, Jahn–Teller (JT) polaron, and tolerance factor.<sup>2</sup> According to Hwang's report,<sup>3</sup> the magnetic properties and magnetoresistance of lanthanum manganite were sensitive to the average La-site cation size. Decreasing the average radius of the La site by rare earth elements Pr and Nd substitution for La, both Curie temperature and the ferromagnetic metal transition temperature decrease. In our recent studies,<sup>4</sup> Nd doping in  $(\text{La},\text{K})\text{MnO}_3$  not only weakens ferromagnetic order, but also induces a structural phase transition and insulator–metal transition at low temperature. These studies imply that the rare earth element might have a contribution to the spin coupling and electronic transport properties. The effect on magnetic and electrical properties of rare earth elements not only depends on their radii size, but also depends on their characteristic properties which will affect the spin fluctuation and spin coupling at low temperature. Here we focus our attentions on the study of the heavy rare earth manganites due to the  $4f$  electron spin antiparallel alignment characterization of the heavy rare earth element, and the motivation in this study is to find out what kind of role the rare earth metal plays in the colossal magnetoresistance materials.

The bulk polycrystalline  $\text{Yb}_x\text{Ca}_{1-x}\text{MnO}_3$  ( $x=0.1,0.2$ ) were prepared by a solid state reaction. The starting materials  $\text{Yb}_2\text{O}_3$ ,  $\text{MnO}_2$ , and  $\text{CaCO}_3$  were mixed in stoichiometric proportions and were calcined at  $1100^\circ\text{C}$  for 24 h. The pow-

der thus obtained was ground, pelletized, and sintered at  $1250^\circ\text{C}$  for 40 h with two intermediate grindings, then cooled to room temperature. The crystal structures of these samples were determined by a Rigaku automatic x-ray diffractometer with  $\text{Cu } K\alpha$  radiation, and refined by Rietveld's method.<sup>5</sup> The magnetization measurements were carried out by a commercial SQUID magnetometer from 4.5 to 400 K under the different applied magnetic fields. The resistivity was measured by means of a standard four-probe method at zero field and 5 T, respectively.

Powder x-ray diffraction (XRD) patterns manifest a single phase with an orthogonally distorted perovskite structure for the two samples as shown in Fig. 1. The related

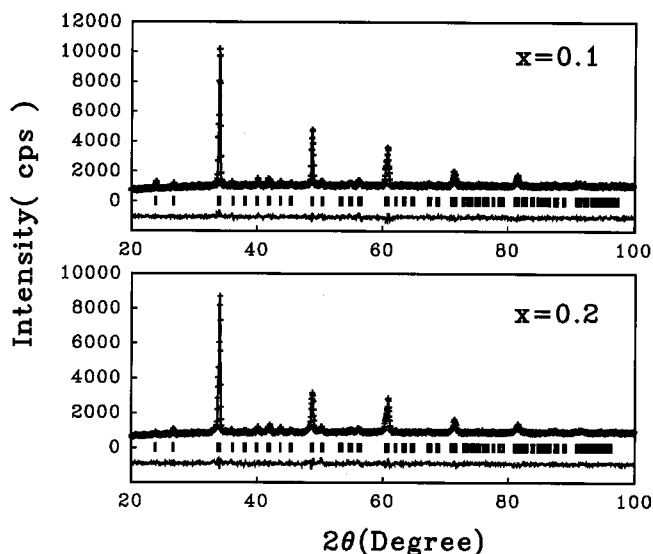


FIG. 1. The powder XRD patterns of  $\text{Yb}_x\text{Ca}_{1-x}\text{MnO}_3$  compounds.

<sup>a)</sup>Electronic mail: nali@physics.siu.edu

TABLE I. The refined structural parameters, coordination of Mn and ionic occupations, the distortion of  $MnO_6$  octahedra and tolerance factor.

| Composition of Yb                   | 0.1  | 0.2                                       |
|-------------------------------------|--|---|
| $a(\text{\AA})$                     | 5.310(6)   | 5.316(4)                                  |
| $b(\text{\AA})$                     | 5.269(3)   | 5.271(3)                                  |
| $c(\text{\AA})$                     | 7.463(8)   | 7.459(7)                                  |
| $v(\text{\AA}^3)$                   | 208.8(6)   | 209.0(3)                                  |
| Ionic occupations                   |  |   |
| (Yb, Ca) $4c(1)$                    | $x, 0.5125(8)$<br>$y, 0.0323(0)$                   | $0.5151(9)$<br>$0.0303(4)$                |
| $O^I 4c(2)$                         | $x, 0.5078(3)$<br>$y, 0.4816(6)$                   | $0.5219(2)$<br>$0.4637(6)$                |
| $O^{II} 8d$                         | $x, 0.1890(3)$<br>$y, 0.2929(6)$<br>$z, 0.0464(7)$ | $0.1857(9)$<br>$0.2996(0)$<br>$0.0493(1)$ |
| $R_p$                               | 3.1%   | 3.5%                                      |
| $R_{wp}$                            | 4.0%   | 4.5%                                      |
| $s$                                 | 1.3  | 1.4                                       |
| Ion-ion and $BL(\text{\AA}) NN$     |  |   |
| Mn-O <sup>I</sup>                   | 1.869,2  | 1.878,2                                   |
| Mn-O <sup>II</sup>                  | 1.874,2  | 1.889,2                                   |
| Mn-O <sup>III</sup>                 | 2.009,2  | 2.010,2                                   |
| $\langle Mn-O \rangle$              | 1.917,6  | 1.929,6                                   |
| $\langle O-Mn-O \rangle (^{\circ})$ | 157.07,6   | 153.11,6                                  |
| Tolerance factor                    | 0.934  | 0.923                                     |

space group is Pbnm, with  $Z=4$ . The lattice parameters increase along  $a$  and  $b$  axes but decrease along  $c$  with increasing Yb content. The unit cell increases with increasing Yb doping. In each unit cell, there are four equivalent crystal positions, i.e., the  $4a:(0,0,0)$ ,  $4c(I):(x,y,1/4)$ ,  $4c(II):(x,y,1/4)$  and  $8d:(x,y,z)$  site, which are occupied by  $4Mn$ ,  $4(Yb,Ca)$ ,  $4O^I$ , and  $8O^{II}$ , respectively. Table I exhibits the refined structural parameters, ionic occupations, and the distortion of the  $MnO_6$  octahedron based on the calculated nearest Mn-O bond lengths and Mn-O-Mn bond angles as well as the tolerance factors.

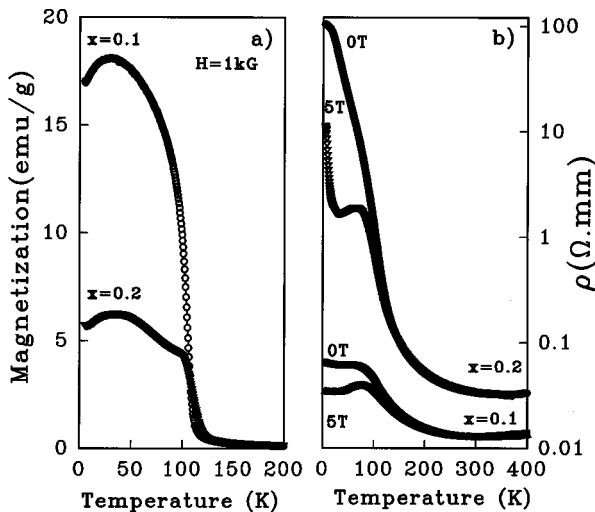


FIG. 2. The temperature dependent magnetization (a) and resistivity (b) of  $Yb_xCa_{1-x}MnO_3$ .

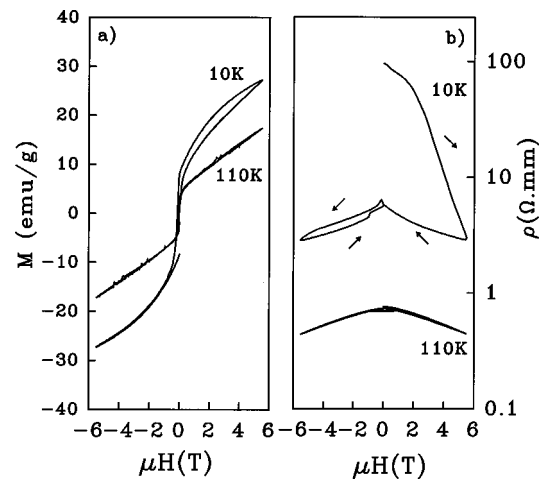


FIG. 3. The applied field dependence of magnetization (a) and resistivity (b) of  $Yb_{0.2}Ca_{0.8}MnO_3$  compound.

The magnetization measurement shows the  $Yb_xCa_{1-x}MnO_3$  are ferromagnetic with the Curie temperatures more than 110 K as illustrated in Fig. 2(a). An asymmetrical magnetization hysteresis loop is found in  $Yb_{0.2}Ca_{0.8}MnO_3$  compound at 10 K with the applied field from  $-5.5$  to  $5.5$  T as shown in Fig. 3(a). This phenomenon is probably due to the magnetocrystalline anisotropy induced by lattice distortion and the heavy rare earth spin coupling at low temperature. There are two aspects of lattice distortion in the context of the magnetic anisotropy of manganites: one is the global strain, which is a general feature for many manganites and determines the anisotropy of the uniform rotation of the spin magnetic moments, and the other one is the alternating local distortion of the  $MnO_6$  octahedron, which will lead to the site-dependence of the magnetic anisotropy energy known as one of the common mechanisms responsible for the noncollinear magnetic order. For the global strain, the corresponding energy changes can be characterized by the site-independent tensor  $\tau$ .<sup>6</sup> Based on our structural refinement, the Yb doping induces the significant shift of the O occupation at  $4c$  crystal position from  $(0.50783, 0.48166, 0.25)$  to  $(0.52192, 0.46376, 0.25)$ . This shift affects the distortion of  $MnO_6$  octahedron. With increasing Yb doping, it shows that both of the Mn-O<sup>I</sup> and Mn-O<sup>II</sup> bonds are extended, the Mn-O-Mn bond angle is bended. Such a distortion of the  $MnO_6$  octahedron will lead to the site-dependence of the magnetic anisotropy energy known as one of the standard mechanisms responsible for the noncollinear magnetic order. If Yb spin coupling has a contribution to the magnetic anisotropy, it is most likely due to the Yb  $4f$  electron spin alignment being antiparallel to  $3d$  electron Mn spin, the long distance  $4f-3d$  spin coupling interaction at low temperature forms ferrimagnetic order and weakens the magnetization as well as induces the magnetic anisotropy.

The temperature dependence of resistivity exhibits different behavior with Yb content. In  $Yb_{0.1}Ca_{0.9}MnO_3$  compound, the zero field resistivity shows a metal-insulator (MI) transition near  $T_C$  and an insulator-metal transition at 301.4 K. The magnetoresistance (MR) ratio decrease with temperature, the MR ratio is only 13% at 100 K. The zero field

resistivity of  $\text{Yb}_{0.2}\text{Ca}_{0.8}\text{MnO}_3$  compound exhibits an insulator behavior in the whole temperature regime. However, an applied magnetic field induced MI transition occurs at 64.8 K with an applied field of 5 T as shown in Fig. 2(b). The magnetic-field-induced IM transition has been found in the previous study in  $\text{Nd}_{1/2}\text{Sr}_{1/2}\text{MnO}_3$  and in  $\text{Pr}_{1-x}\text{Ca}_x\text{MnO}_3$  crystals.<sup>7,8</sup> The explanation can be described as the following. In accord with its magnetization behavior, the resistivity shows phase transition from antiferromagnetic charge ordered insulating state to the ferromagnetic metallic state which is caused by application of an external magnetic field. From the thermodynamic point of view, both states are almost energetically degenerate, but the free energy of the ferromagnetic state decreases by the Zeeman energy  $M_s H$  ( $M_s$  is the spontaneous magnetization) so that the magnetic-field-induced transition would occur by applying an external magnetic field of a few Tesla. This destabilizes the antiferromagnetic charge ordered state and drives the phase transition to the ferromagnetic metallic state.<sup>7</sup>

It is interesting that a huge asymmetrical field dependent resistivity hysteresis loop at 10 K is observed in  $\text{Yb}_{0.2}\text{Ca}_{0.8}\text{MnO}_3$  compound as illustrated in Fig. 3(b). However, this hysteresis loop is melting with temperature and totally disappears near  $T_C$  temperature. In general, if the spin-dependent scattering at the magnetic domain boundaries is totally responsible for the observed MR, the MR magnitude will be scaled by the square of the spin-polarization of the carriers, namely,  $(M/M_s)^2$  (where  $M_s$  is the saturation magnetization).<sup>9</sup> In our experiment, the relationship between MR and magnetization square is not linear, but both magnetization and resistivity hysteresis loops of  $\text{Yb}_{0.2}\text{Ca}_{0.8}\text{MnO}_3$  compound exhibit the asymmetric behavior. The charge ordering and magnetic anisotropy, which is induced by lattice distortion and the heavy rare earth spin coupling at low tem-

perature, behave in an antiferromagnetic or ferrimagnetic insulating state, but these insulating states melt with an applied magnetic field. The resistivity shows the transition from antiferromagnetic or ferrimagnetic insulating state to canted ferromagnetic metal or ferromagnetic metal state that occurs with a large applied magnetic field. The magnetic-field-induced IM transition in  $\text{Yb}_{0.2}\text{Ca}_{0.8}\text{MnO}_3$  compound appears to be irreversible.

In conclusion, the  $\text{Yb}_x\text{Ca}_{1-x}\text{MnO}_3$  crystallizes in an orthogonally distorted perovskite structure, and exhibits the ferromagnetic order. The  $\text{Yb}_{0.2}\text{Ca}_{0.8}\text{MnO}_3$  compound shows a very complicated magnetization and resistivity behavior. A magnetic-field-induced IM transition has been found in this compound and the huge asymmetric magnetization and resistivity hysteresis loops have been observed at 10 K, which might be interpreted by the charge ordering and magnetic anisotropy.

This work is supported by CARS-University of Chicago. XRD work, carried out in the Center for Microanalysis of Materials, was partially supported by the U.S. Department of Energy under Contract No. DEFG02-ER45439.

<sup>1</sup>S. Jin, T. H. Tiefel, M. McCormack, P. A. Fastnacht, R. Ramesh, and L. H. Chen, *Science* **264**, 413 (1994).

<sup>2</sup>A. J. Millis, *Nature (London)* **392**, 147 (1998).

<sup>3</sup>H. Y. Hwang, S.-W. Cheong, P. G. Radaelli, M. Marezio, and B. Batlogg, *Phys. Rev. Lett.* **75**, 914 (1995).

<sup>4</sup>Y. Q. Guo, R. Waeppling, X. H. Zhang, and N. Ali (unpublished).

<sup>5</sup>H. M. Rietveld, *J. Appl. Crystallogr.* **2**, 65 (1969).

<sup>6</sup>O. K. Anderson, *Phys. Rev. B* **12**, 3060 (1975).

<sup>7</sup>P. Schiffer, A. P. Ramirez, W. Bao, and S. W. Cheong, *Phys. Rev. Lett.* **75**, 3336 (1995).

<sup>8</sup>Y. Tomioka, A. Asamitsu, Y. Moritomo, and Y. Tokura, *J. Phys. Soc. Jpn.* **65**, 3626 (1995).

<sup>9</sup>J. Q. Xiao, J. S. Jiang, and C. L. Chien, *Phys. Rev. Lett.* **68**, 3749 (1992).